Three-dimensional digitization of highly reflective and transparent objects using multi-wavelength range sensing

M. F. Osorio · A. Salazar · F. Prieto · P. Boulanger · P. Figueroa

Abstract Digitizing specular and transparent objects pose significant problems using traditional 3-D scanning techniques due to the reflection and refraction that interfere with the optical scanning process used for triangulation. In this paper, we present how one can digitize those difficult objects by modifying a commercial 3-D acquisition system with an interchangeable ultraviolet and infrared light source. Experimental results show that the proposed technique can generate accurate 3-D models of these optically challenging objects without major modifications to the 3-D scanner. The results were obtained without preprocessing or multi-view manipulations. The precision of the 3-D measurements is evaluated relative to the visible spectrum acquisition obtained by painting the test objects with matte paint to suppress optical difficulties. Results shows that wavelength changes in the 3-D acquisition system do not change the scanner precision but solve many of the issues that specular and transparent objects poses.

M. F. Osorio · A. Salazar
Universidad Nacional de Colombia sede Manizales,
Cra 27 No. 64-60, Manizales, Caldas, Colombia

F. Prieto (✉)
Universidad Nacional de Colombia sede Bogotá,
Carrera 30 No. 45-03, Bogotá, Colombia
e-mail: faprietoo@unal.edu.co

P. Boulanger
University of Alberta, 2-32 Athabasca Hall,
Edmonton, Canada

P. Figueroa
Universidad de los Andes, Carrera 1 No. 18A-10,
Bogotá, Colombia

1 Introduction

There are several commercial three-dimensional (3-D) scanning devices [1,2] with sufficient resolution and speed that are used today in numerous fields such as industrial design, manufacturing automation, archeology, art restoration, intelligent robotics, and much more. Many of these devices are based on the active triangulation and tends to be very sensitive to the optical properties of the object's surface been digitized. One can classify the optical properties of many objects as homogeneous and inhomogeneous. Inhomogeneous or Lambertian objects are characterized by being uniformly reflective due to the randomness of the surface microstructure. Many of real-world objects do not follow the uniformly reflective assumption as the surface optical properties may vary wildly. These homogeneous objects are characterized by even surface properties as the surface maybe specular due to a more uniform micro-structure, maybe transparent or maybe translucent. The surface albedo may also vary wildly.

In commercial and research 3-D digitizing systems, the main assumption is that the object's surface is opaque and Lambertian. Geometrical digitization of highly reflective, translucent, transparent or, in general, homogeneous materials is recent and requires complex optical setups to solve the various problems [3]. There is a need in automotive and other manufacturing industries to digitize surfaces with high reflectivity and high transmissivity for quality control or recording. Using standard commercial 3-D scanner on those objects usually produce saturations, shadows, inter-reflections, total transmission, and other variations difficult to predict [4]. The usual way to solve this problem is to cover the surface with a Lambertian reflective coating like talcum or matte paint. But in many situations, this solution is impossible. Another solution is to take numerous views of the object hoping for some light to come back to the sensor that would allow 3-D

triangulation but in many cases one can only retrieve only partial 3-D data from the object's surface.

This paper proposes a non-invasive technique for the acquisition of several specular objects such as ceramic and metals or transparent objects like glasses and plastics. The proposed technique is based on the optical triangulation using a long-wave ultraviolet light source for specular objects, or short-wave infrared source for transparent and translucent objects. Since optical properties of object surfaces varies with wavelength, one can use multi-spectral 3-D acquisition to counteract the adverse effects produced by the high reflectivity or high transmissivity. Using multi-spectral lighting in the 3-D acquisition process, we will demonstrate that it is not necessary to perform additional steps in reconstruction or invasive manipulation of an object in order to get excellent 3-D measurement.

The remainder of this paper is organized as follows. An overview of related work concerning the 3-D acquisition of optically challenging objects is presented in Section 2. Section 3 presents a physical model of specular, transparent and translucent surfaces as a function of wavelength. A description of the proposed 3-D acquisition system and the experimental results are presented in Section 4. We will then conclude and discuss future possibilities of this work in Section 5.

2 Literature review

This section presents an overview of the principal techniques and systems used to digitize 3-D objects with highly reflective or transparent surfaces. One can find in [3] an excellent review of the relevant literature.

2.1 Highly reflective objects

Several methods for measuring specular objects have been proposed. One of the most common methods is to project a known pattern of light on the object's surface. The light pattern is distorted by the effect of specular reflections and its 3-D shape. The shape is recovered by observing the smooth distortion of the original pattern on the object; this process is called shape from distortion [5–8]. To represent the distortion, Tarini [5] uses an environment mapping technique [9] to represent the optical interactions between an object's surface and its light sources (the projected pattern). A 3-D shape estimate is performed using a phase-shift algorithm based on a single camera observation. Since the 3-D shape reconstruction is generally impossible from just one image, they used iterative multi-view integration to estimate the complete object shape. This techniques include alignment [10,11], view-merging [12,13], and model simplification [14]. Adato [8] uses the specular flow from the relative

motion, between the specular object and its environment, in order to reconstruct shape geometry of specular objects. A pair of coupled nonlinear partial differential equations, relating specular flow to the surface, must be solved. Although the solution of these equations in general is difficult, authors show that in some cases the equations become a system of decoupled linear equations.

Direct ray measurements are methods that measure two points of a light beam from the light source to a surface point. Kutulakos et al. [7,15] developed an algorithm in which they assume that one reflection event exactly occurs along the ray. Measuring the reflected and the observed ray, a surface position and its associated normal direction are recovered at every pixel. The 3-D shape of specular and transparent objects could be recovered by three viewpoints if incoming light undergoes two reflections or refractions. They used an environment mapping procedure [16] for finding correspondence between the image and the display. Bonfort et al. [6] present a detailed description for shape reconstruction with direct ray measurements using a single camera viewpoint and the reflection of a planar target placed at the two different positions. They also show how one can apply this technique to arbitrary surfaces.

Park and Kak [17] present a 3-D reconstruction method for modeling specular objects. They introduce the concept of multi-peak range imaging by considering the effects of inter-reflections which creates multiple peaks in the range sensor. The basic idea is to store multiple measurements of range for all existing peaks and to ensure that one of them is an object point that corresponds to a true illuminated point. The false measurements caused by mutual reflections are eliminated by iteratively testing if local smoothness and global consistency are preserved. In Park [18], the method is improved by performing changes in the tests applied to evaluate the effects of the parameters used. The elimination process of false measurements is achieved in two stages. To evaluate the performance of the method, the objects were painted with matte paint to obtain a 3-D reference by eliminating the optical problems. The experimental results indicate an improvement over traditional methods but the computational cost is high compared to other techniques because the tests must be performed on a considerable number of images.

2.2 Transparent and translucent objects

Transparent objects are those that allow light the pass through them, such as water and glass. Those objects are difficult to digitize with the standard techniques because most of the light that comes to its surface is refracted, and only a small portion is reflected. For the acquisition of transparent objects, there are numerous methods based on polarization [19], using silhouettes detection [20], using movement detection [21], and using patterns projection. [22].

Miyazaki et al. [19] propose a method using a camera equipped with a polarizing filter. They obtain the normal of the object surface from the degree of polarization of each point on the surface, which depends on the light incidence angle. In order to obtain the correspondence between the degree of polarization and the normal of the surface, polarization measurements at two positions are compared; one position in the normal direction and the other for a small inclination. Chen et al. [23] present a technique based on a combination of polarization and change of phase using structured light. The change of phase of the light patterns to higher frequency allows the separation of the reflection into its diffuse and specular components. Analyzing two polarized images orthogonally, the effects of multiple dispersions are removed and thus the geometry of the object can be computed. Although the results are quite acceptable, the high cost the acquisition devices makes this technique difficult to implement without adding expensive equipment to the digitizing hardware.

The system proposed by Matusik et al. [20] consists of a set of cameras and light sources (a monitor projecting color patterns). The objects are placed on a turntable. With this system, an object is digitized and modeled using the captured reflectance fields. Yamazaki et al. [24] propose a method to acquire the surface of transparent objects by using a screen with two phase changes and two cameras.

Hullin et al. [25] propose a method for transparent object acquisition by submerging the object into a fluorescent liquid, and then projecting a laser beam that will become visible to CCD camera. In this system, the light rays that are analyzed are those that become visible due to fluorescence and not to surface reflections. In this way, intersection points between the laser beam and the surface of the object can be measured.

The previous techniques for the 3-D acquisition of specular, transparent, and translucent objects require specialized and expensive hardware or major change to the standard 3-D digitizing software. In comparison, the proposed solution only requires the modification of the illumination source of a Vivid i9 3-D scanning system. The main idea here is that under different wavelength the optical properties of an objects becomes very different. For very reflective objects ultra-violet (UV-A) light is used to reduce the specular component and for transparent objects Infrared (IR $\lambda = 1,000$ nm) is used to increase its reflectivity.

3 Multi-spectral 3-D scanning

The acquisition technique introduced in this paper uses a commercial active triangulation system based on structured light by Minolta (Vivid i9 System). In this section, a brief explanation on how the triangulation system works is presented. In addition, in order to understand the relevance of
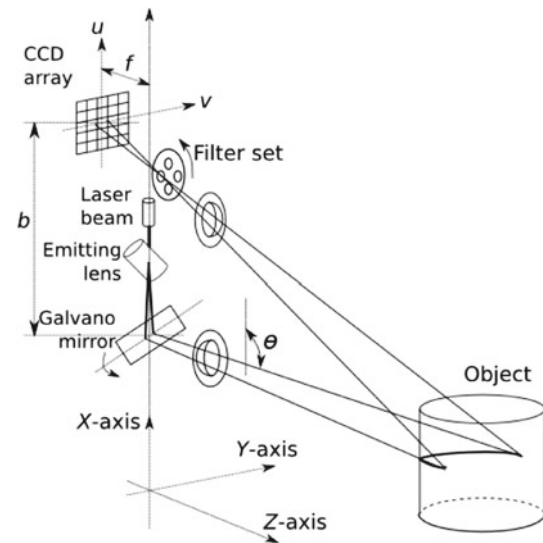

Fig. 1 Triangulation principle and main hardware components of the Vivid 9i system

using multi-wavelength lighting in the acquisition process, an analysis of the optical characteristics of materials from a physical viewpoint is also presented.

3.1 Triangulation method

The triangulation principle of the Vivid 9i system is based on the most commonly used method to acquire 3-D information using optical devices [26,27]. It is an active stereoscopic technique where the distance of the object is computed by mean of a directional light source and a CCD camera's 2D array. The Vivid 9i system uses a class 2 (red) laser with a wavelength of 690 nm (in the visible spectrum). The laser beam is spread out as a light-stripe through a cylindrical lens. The emitted horizontal stripe light is then deflected from a Galvano mirror and projected to the scanning object. The object's surface, usually opaque and Lambertian, scatters the light, which is then collected by a CCD camera located at a known baseline distance from the laser (see Fig. 1). The CCD camera's 2D array captures the surface profile's image by recording the pattern change [28], and digitizes all data points along the laser line. This process is repeated by scanning the stripe light vertically on the object surface using a Galvano mirror, to obtain a 3-D image data of the object [29].

By trigonometry, the 3-D spatial (X, Y, Z) coordinates of a surface point are computed, related to a coordinate system located in the optical center of the sensor using Eq. 1 (Fig. 1):

$$(X, Y, Z) = \frac{b}{f \cos \theta - u} (u, v, f), \qquad (1)$$

where b is the baseline or distance between the optical centers of the projector and the camera, f is the focal distance of the camera lens, u and v correspond to the position of the

point in the plane of the image, and θ is the projection angle of the beam in relation to the x-axis.

3.2 Optical properties of objects

The optical properties of the object's surface to be digitized determine significantly the performance of the capture device. It is well know that whenever a ray of light is incident on the boundary separating two different media, part of the ray is reflected back into the first medium and the remainder is refracted into the second medium. The reflectivity of a surface is the property that determines the fraction of incident light reflected back to the CCD sensor.

3.2.1 Highly reflective objects

Given a light source, a surface, and an observer, the reflectance model describes the intensity and spectral composition of the reflected light that will reach the sensor. The intensity of the reflected light is determined by the intensity and wavelength of the light source, and the behavior of the surface at such wavelength [30]:

$$R = \frac{I_R}{I_0} = \frac{(n-1)^2 + k^2}{(n+1)^2 + k^2}, \tag{2}$$

where R is the reflectivity, I_R is the reflected intensity, I_0 is the incident intensity, n is the refractive index and k is the absorption constant. For materials like metal n depends on the wavelength (λ) of incident light:

$$n = n(\lambda). \tag{3}$$

The reflectance also depends on how the surface absorb light and is called surface albedo. Surfaces can be classified into Lambertian (diffuse) and non-Lambertian (specular) surfaces. A Lambertian surface is a surface that only has diffuse reflectance, i.e., reflects light in all the directions. The reflected light intensity is proportional to the brightness of the incident light, the surface albedo, and the surface area of the element seen from the light source (small area) [31]. A specular surface has the property that the incident light and the reflected light have the same angle in relation to the normal of the object surface.

In contrast to a diffuse surface, the intensity of the reflected light captured by the CCD on a specular reflection depends on the position of light sources, and the viewpoint of the CCD. With highly reflective surfaces such as metals or ceramics, the reflection of light tends to be specular. When light is projected on these surfaces, maximum points of light are generated. These peaks of light saturate the camera sensor, making the 3-D acquisition process almost impossible.

3.2.2 Transparent and translucent objects

The relative speed of the light that goes through material is expressed by the refractive index n. The refractive indexes for the light that passes from a transparent material with index n_i to another one with index n_r are related to the angles of incidence and refraction, according to the Snell law (Eq. 4):

$$n_i \sin \theta_i = n_r \sin \theta_r. \tag{4}$$

Refraction is generally accompanied by a weak reflection produced at the surface that limits the two transparent materials. The beam, when arriving at that surface boundary, is partly reflected and partly refracted, which implies that the reflected and refracted beams will have less light intensity than the incident ray. This distribution of intensity takes place in a proportion that depends on the characteristics of the transparent material in contact and the angle of incidence in relation to the surface. As a consequence, the magnitude of the refractive index determines the material appearance.

3.3 Optical properties versus wavelength

From optical properties of objects, we conclude that reflected light depends on the refractive index, which, as stated in Eq. 3, also depends on the wavelength of light. The proposed technique in this paper for the digitalization of specular or transparent object, is based on the modification of their refractive index using an ultraviolet or an infrared light source.

The interaction between light, from an external source, and the electronic structure of a material creates multiple optical phenomena such as absorption, transmission, reflection, and refraction. In any of these cases, the energy of the light changes, as a consequence of the refractive index change, producing refraction.

3.3.1 Highly reflective objects

The particularities of light reflection from specular surfaces are due to the presence of a large number of electrons that are weakly connected with their own atoms. These electrons can be considered almost free. Since the density of free electrons is high, even very thin layers of metal reflect most of the incident light and in general, they are practically opaque. With UV light, optical properties of metal depend mainly on the behavior of the bound electrons, that are characterized by their own frequency located in the zone of shorter wavelengths. The participation of these electrons determines the so-called non-metallic optical properties.

Figure 2 shows the reflectance behavior of four different types of metals (silver (Ag), gold (Au), copper (Cu), and aluminum (Al)) in the presence of light with wavelengths ranging from 200 to 1,100 nm. The behavior of these surfaces in the UV-A range (315–380 nm) have the lowest reflectance
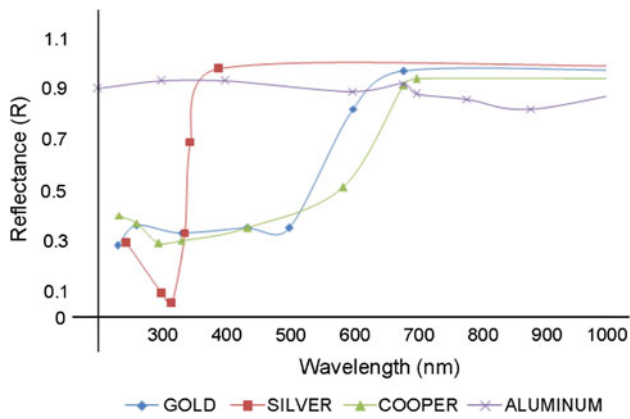
Fig. 2 Reflectance versus wavelength for Au, Ag, Cu and Al [32]

Table 1 Metals Reflectance with $\lambda = 350\,\text{nm}$

Material	R (%)
Gold (Au)	34.3
Silver (Ag)	67.2
Copper (Cu)	31.6
Aluminum (Al)	90.3

values. This means that in this wavelength range, specular properties of metallic objects can be controlled and reduced significantly. The behavior of some metals at a wavelength $\lambda = 350\,\text{nm}$ (UV-A) are summarized in Table 1. One can see at Table 1 and at Fig. 2, that for those wavelength the percentage of reflectance is lower. This means that during the acquisition of highly reflective objects, it is possible to significantly reduce disturbances caused by regions with a high reflectance values, if the light source is changed from the visible to a UV-A.

3.3.2 Transparent and translucent objects

Transparency is a property of transparent materials which deals with the optical transmission defined by the Beer–Lamberts law (Eq. 5):

$$\frac{I}{I_0} = e^{-\alpha x}, \tag{5}$$

where I_0 is the intensity of the beam that enters the material volume with a depth x; I is the intensity of the emergent ray, and α is the absorption coefficient, defined by (Eq. 6):

$$\alpha = \frac{4\pi}{\lambda} K(\lambda), \tag{6}$$

where $K(\lambda)$ is the absorption index, which depends on the wavelength λ [33].

Figure 3 illustrates the behavior of the transmission property of standard glass materials in the IR range ($\lambda > 750\,\text{nm}$). As observed, for each of these compounds there exists a
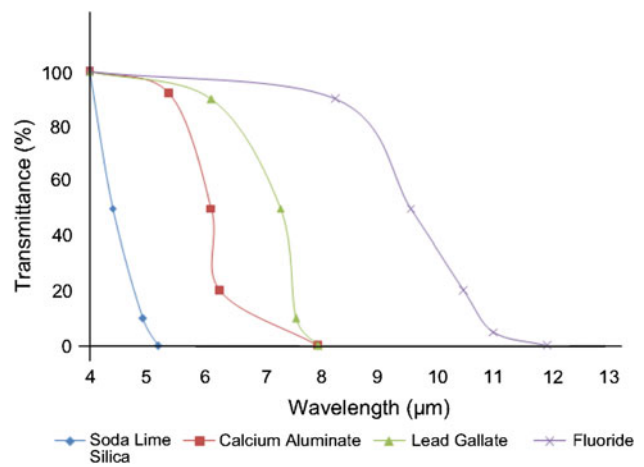

Fig. 3 Transmittance versus wavelength the IR Range [32]

wavelength value where the transmission is 0%. For wavelengths superior to 1,000 nm, glasses can be considered opaque. In this way, the problem of total light transmission for normal illumination conditions, can be solved and used for 3-D scanning.

4 Experimental results

In this section, we will present the system develop to solve the problem of 3-D acquisition of transparent and specular objects. As we stated, the idea is to illuminate the object in order to affect its optical properties. For specular objects, we use ultraviolet light while for transparent objects we use infrared light.

In this work, we focus on the acquisition problem, so for registration of the views and reconstruction process, we use a standard software such as Geomagic. Initially, the clouds of points are registered until a whole part is obtained; then, the reconstruction software generates a triangulated model of the part.

4.1 The acquisition system

The acquisition system is composed of a commercial 3-D scanner (Minolta Vivid 9i), an illumination source, and a turntable (see Fig. 4). The light source is a UV-A lamp of 20 W and is used to digitize specular objects. The light can then be replaced by an IR lamp with a maximum spectral peak located at 1,000 nm where transparent and translucent objects can be digitized. This is possible because the Vivid scanner uses light-stripe method where a horizontal light stripe is projected on the object's surface by using a galvano mirror. The reflected light from the object is measured by the CCD sensor and then converted into distance information by applying the triangulation calculation. It is well known that the CCD sensors have a peak sensitivity in the visible spectrum and has a relatively low sensitivity in the UV and high-IR range.
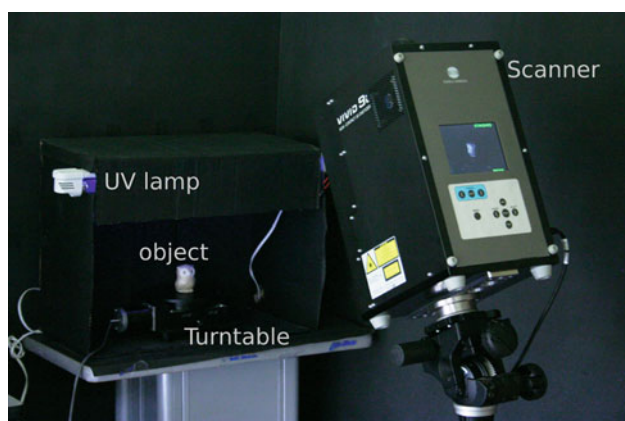
Fig. 4 Acquisition system

This effect can be compensated by increasing the intensity of the light source or by changing the CCD to another technologies that are more sensitive to UV or IR. For simplicity, we have decided to keep the CCD and to simply increase the light intensity to compensate for the reduced sensitivity. Technologies based on Gallium Arsenide (GaAs) can significantly increase the sensitivity of the imaging sensors to IR but at great cost as most GaAs sensors are ten times more expensive than its CCD counterpart. Other technologies such as phosphore coated CCD [34] may reduce the cost of IR imaging sensor but are limited to wavelength between 1,200 and 1,600 nm. To increase the sensitivity of CCD sensors in the UV range, a process called backside thinning (BST) [35] is used in which the backs of the sensor is thinned to extend the wavelength range of the sensor from the visible to the UV. Already, a number of different approaches to BST have been proposed by Sarnoff, Fairchild, and the Jet Propulsion Laboratory to improve the sensitivity of both CCD and CMOS imagers in the UV region. For different spectral responses to cover the entire wavelength of ultraviolet (UV), visible, and infrared (IR), different types of sensors have to be built. Novel multi-spectral sensors based on patented technologies from Banpil Photonics [36] are very promising.

The acquisition system geometry was set up as following:

1. The ambient light conditions are controlled by locating the object into a dark room;
2. The light sources used (UV-A or IR) was located above the object;
3. The object is placed on the turntable;
4. The object is then digitized using the light-stripe system.

4.2 Digitalization process

Acquisition was performed for many test objects, with a variety of kinds of surfaces: silver metals, golden metals, ceramics, transparent and translucent objects. The objects
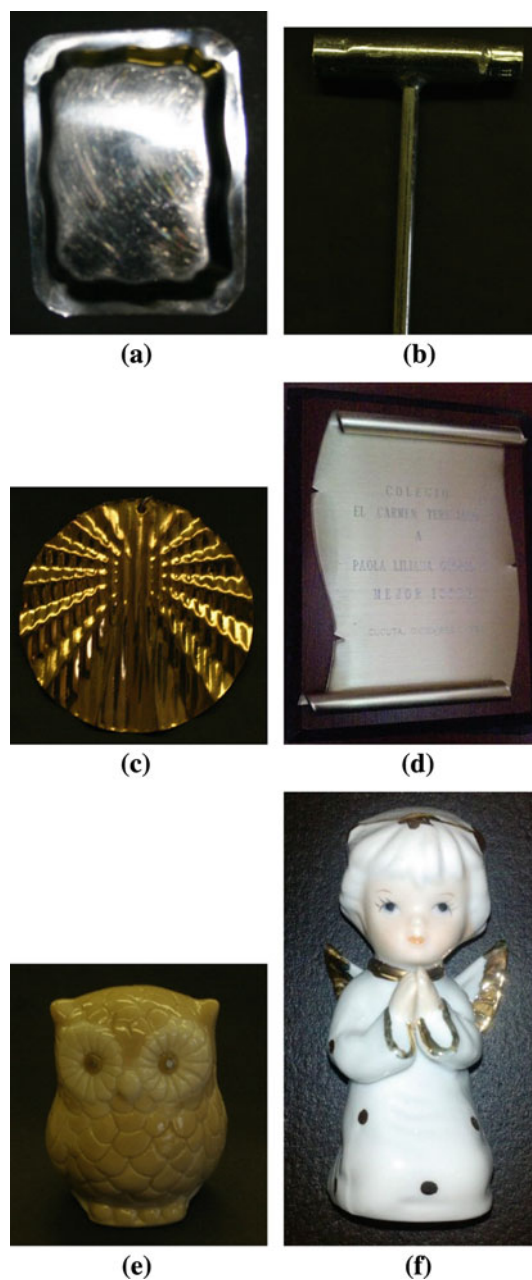

Fig. 5 Some highly reflective objects. **a, b** Silver metal; **c, d** Golden metal; **e, f** Ceramics

dimensions were in the range $[5 \times 5 \times 5 \text{ cm}, \ 12 \times 12 \times 12 \text{ cm}]$, but for other dimensions we only need to change the camera lens and re-calibrate.

4.2.1 Highly reflective objects

Figure 5 shows some of the specular object used to show the performance of the acquisition system when a UV light is used.

Fig. 6 Range images of the
three acquisition methods.
a, **d** White light; **b** UV-A light;
c, **f** Painted object; **e** IR light
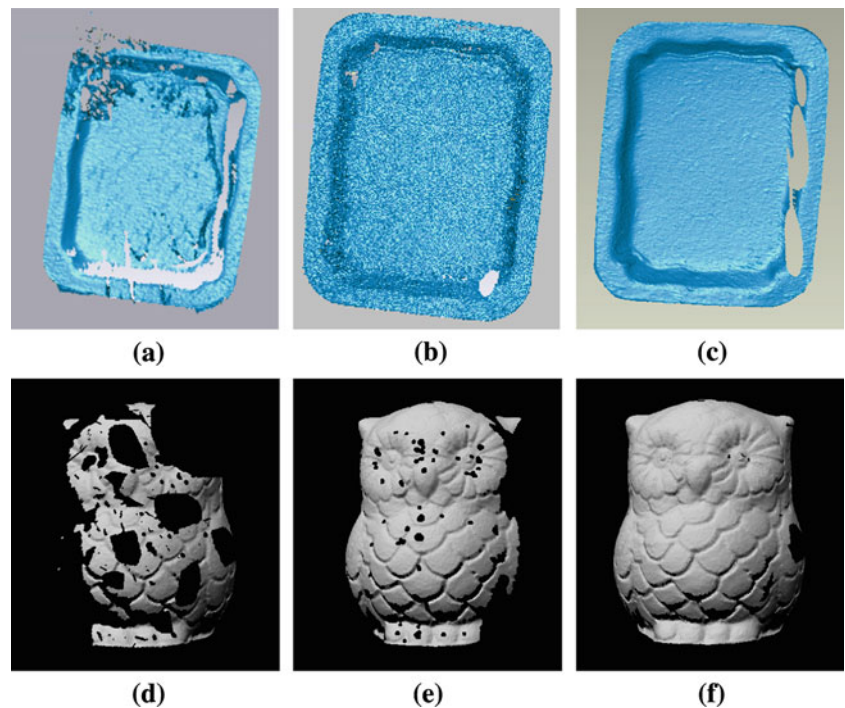
For each object, three acquisitions were performed: one by illuminating the object with white light, another with UV-A and the last one using again white light but where the object is now painted white matte paint to eliminate reflectivity issues. The last acquisition is used as the ground truth acquisition, in order to measure the error of the others acquisitions.

Figure 6 shows some results for the three acquisitions. The absence of information and erroneous information in the visible light acquisition compared with the other two acquisitions is obvious. One can observe that the acquisitions using the proposed illumination method produce 3-D data that are much closer to the ideal situation where the object is painted.

In order to reconstruct a full model of an object like the one in Fig. 5a, many views were to be acquired. These views where then registered and the CAD model obtained using a standard software. Figure 7 shows the reconstruction result for a silver metal object. For a full reconstruction, six views are required when white light is used, against four views when the UV-A light is used. Evidently, the acquisition using UV light outperforms the acquisition using white light. In addition of that, better geometry and smoother data can be measured when the UV-A light is used.

A comparison between the objects reconstruction using the proposed lighting and the painted object (ground truth) is performed and shown at Fig. 8. It was obtained after we registered the two models and measured the distance between the closest points on each mesh. The color reference on the left of each figure represents the magnitude of the distance (absolute error). Being greater negative in blue and greater positive in red. One can see that the reconstructed objects
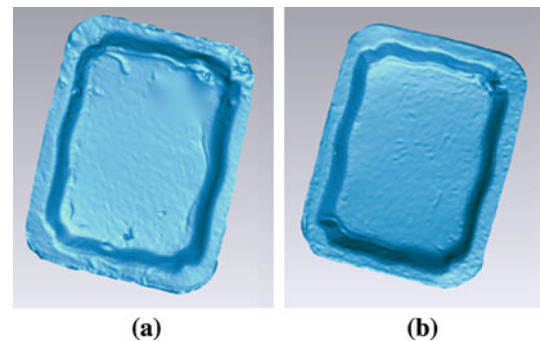

Fig. 7 3-D model of the part of Fig. 5a. **a** White light; **b** UV-A light

fit well with an average reconstructions error of 0.034 mm relative to the painted object. The maximal error was of 0.083 mm and was obtain for the comparison illustrated in Fig. 8d.

The information obtained after applying the proposed method is quite close to the one obtained from the ground truth. The differences between the two models are mostly located at the borders of the scanning region and are probably due to the acquisition angle. To evaluate the relevance of the position of the scanner regarding to the object, acquisition was performed by moving the scanner at different angles relative to the object (each 15°), acquiring the same view in each case. Table 2 shows the number of obtained triangles in each view with the different scanner orientations. Clearly, when the orientation is closer to normal direction between the scanner and the object (0°), a greater number of triangles are obtained. One can see that when the scanner is not at the
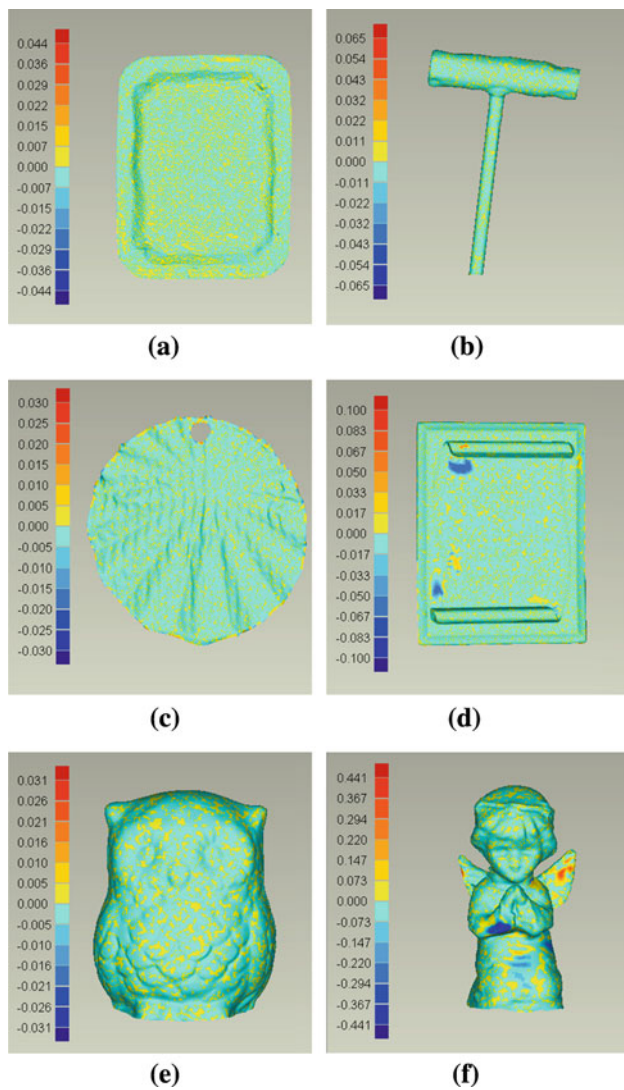
Fig. 8 Comparison of the results between the proposed method and the ground truth

Table 2 3-D acquisition from different angles (Fig. 5a)

Angle	# Triangles
75°	152048
60°	234797
45°	285552
15°	343511
0°	389947
−15°	277824
−45°	225903
−60°	150217
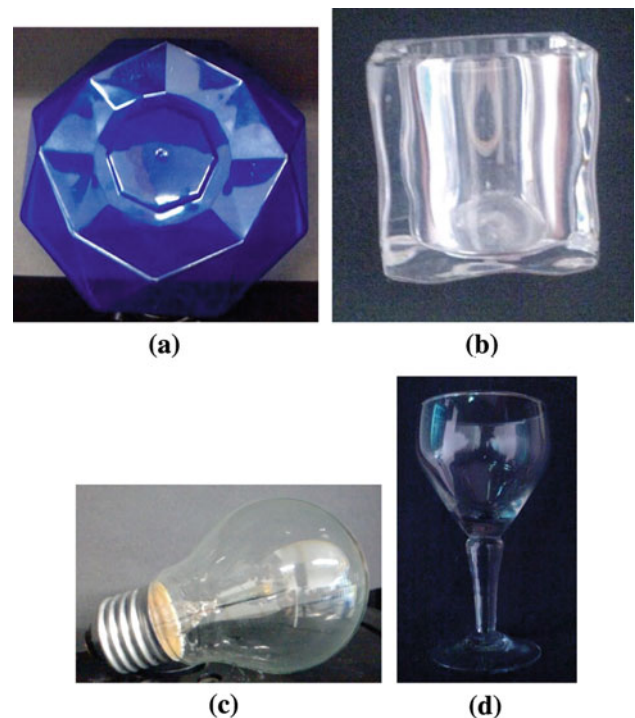
Fig. 9 Some translucent and transparent objects. **a**, **b** Translucent; **c**, **d** Transparent

normal orientation of the object, the amount of information captured by the sensor decreases.

4.2.2 Transparent and translucent objects

The digitalization process for these objects is similar to the one for the digitalization of specular objects. For illustrate this process, we use objects like the ones presented in Fig. 9.

Again, for each object, the three mentioned acquisitions were performed. For the second acquisition, contrary to the specular object, translucent and transparent objects were illuminated with IR light. Figure 10 shows some results for the three acquisitions acquisition mode: visible light, IR light, and the painted object.

It is remarkable the absence of information in the visible light acquisition compared with the other two acquisitions.

As a consequence of this lack of information, it is almost impossible to reconstruct a full model of a transparent or a translucent object when it is not used special hardware or software. Figure 11 shows the final reconstruction of two objects when they are illuminated with IR light, the comparison with the acquisition using white light cannot be done because, as already mentioned, it is not possible to acquire the surface geometry with this type of light.

Finally, as for the case of highly reflective objects, we present at Fig. 12a comparison between the objects reconstruction using the IR light and the painted object (ground truth). The two reconstructed objects fit well with an average error of 0.287 mm, and a maximal error of 0.699 mm obtained for the comparison illustrated in Fig. 12c.

Fig. 10 Range images of the three acquisition methods for transparent and translucent objects. **a, d** White light; **b, e** IR light; **c, f** Painted object
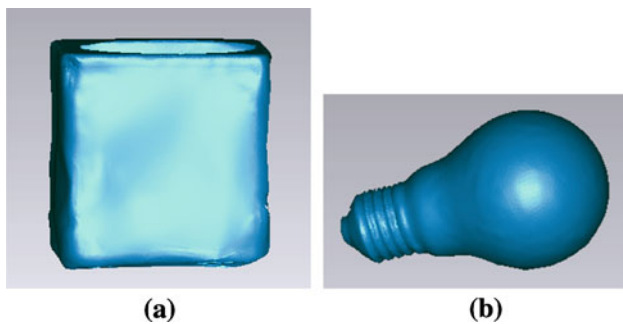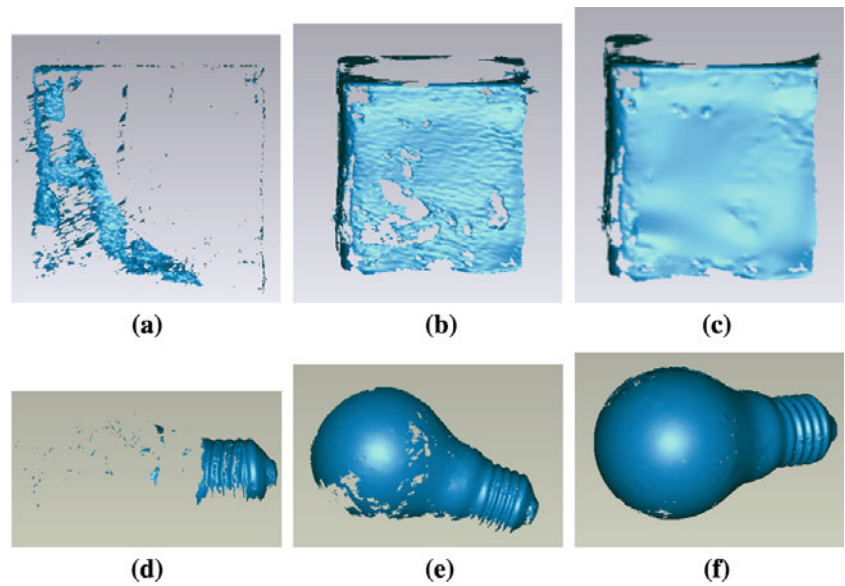

(a)

(b)

(c)

(d)

(e)

(f)

(a)

(b)

Fig. 11 3-D Reconstruction using IR light. **a** Translucent; **b** Transparent

4.3 Comparison of the proposed technique

In addition of the acquisition evaluation realized between the proposed technique and the ground truth (painted object), we summarize in Table 3 the principal result reported in literature.

We observe that, contrary of the proposed technique, reported techniques require the use of a special hardware or software. Although we propose the use of a special illumination, this required hardware is non invasive, non expensive and of easy manipulation. Table 3 also shows the required number of acquisition views for a whole reconstruction is, in most of the times, smaller when the proposed technique is used.

Related to the reconstruction global error, for specular objects it is minor when the proposed technique is used. For transparent or translucent objects, even if the error obtained using the proposed method is not smaller, it is not far from others techniques. Additionally, the non-invasion property of the technique is an important point for digitalization of bigger objects.
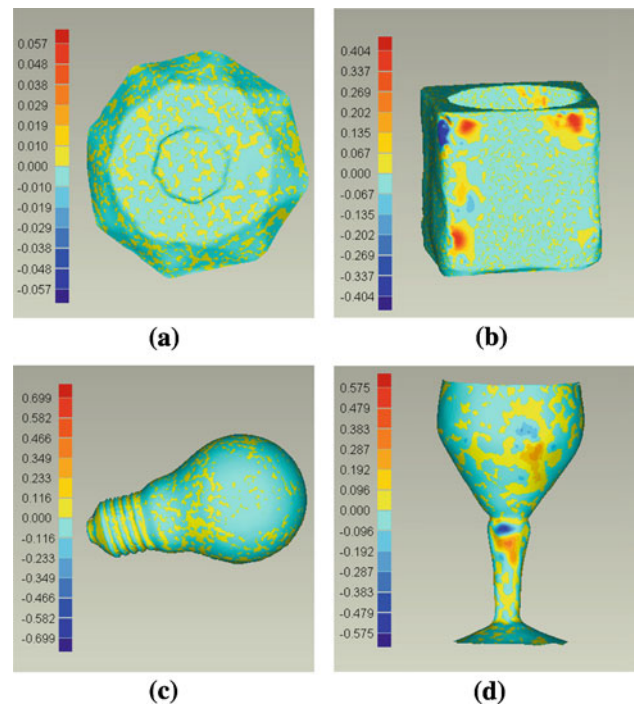

(a)

(b)

(c)

(d)

Fig. 12 Comparison of the results between the proposed method and the ground truth. **a** Comparison part Fig. 9a; **b** Comparison part Fig. 9b; **c** Comparison part Fig. 9c; **d** Comparison part Fig. 9d

5 Conclusion and future work

Three-dimensional digitization of highly reflective, transparent and translucent objects is a difficult problem in computer vision. Many systems based on triangulation that use lighting in the visible spectrum cannot really solve this problem. This paper proposes a new method for digitizing accurate 3-D models of objects that have challenging optical properties using a standard projected light stripe method

Table 3 Comparison of reported techniques

Technique	Type of surface	Size	Hardware	Software	Number of views	Global error (RMS)
Proposed technique	Metallic–Ceramic (Specular)	10 × 8 cm	Scanner Vivid 9i Minolta and UV light (non invasive)	Geomagic Studio (standard reconstruction software)	4 (Met.)–5 (Cer.)	0.007 mm (Met.)–0.005 mm (Cer.)
Phase-shift method—Yamazaki et al. [24]	Planar mirror (Specular)	15 × 10 cm	Two Nikon CCD cameras (3008 × 2000 pixels, a 28 mm lens) and DELL PC display (non invasive)	Special software similar to tomographic reconstruction	–	0.22 mm
Multipeak range imaging—Park et al. [18]	Ceramic (Specular)	–	Camera and Laser projector (non invasive)	Modified ICP algorithm, local test and global test	18	–
Shape-from-distortion—Tarini et al. [5]	Mirroring object (Specular)	6 cm (diameter)	Sony CRT monitor and Kodak DCS 560 digital camera (non invasive)	Algorithm to acquire an environment matte that captures with sub-pixel precision	–	0.021 mm
Proposed technique	Glass (Transparent)	11.5 × 6 cm	Scanner Vivid 9i Minolta and IR light (non invasive)	Geomagic studio (standard reconstruction software)	9	0.287 mm
Light-path triangulation—Kutulakos et al. [15]	Glass (Transparent)	13 × 23 cm	Sony DXC-9000 video camera (720 × 484-pixel) and DELL LCD display (non invasive)	Algorithm pixel-to-point based on "environment matting"	5	0.644 mm
Shape-from-distortion—Hullin et al. [25]	Glass (Transparent)	4.32 cm (diameter)	Laser projector, CCD camera and glass tank containing a fluorescent liquid (invasive)	Surface detection algorithm	–	0.046 mm

where the lighting source is in the visible range for Lambertian regions, IR range for transparent regions, and UV-A range for specular regions. By combining, those three wavelength one can digitize optically difficult objects accurately and completely.

The proposed system uses a commercial 3-D scanner (Minolta Vivid i9) with modified light sources to acquire range data. This type of lighting reduces the adverse effects caused by the reflective or refractive phenomena produced when visible light is used. The UV-A wavelength has the property to reduce the brightness of specular surface measured by the CCD sensor. In contrast, IR light reduces the refractive effect and increases the reflectivity of the surface allowing the CCD sensor to measure a signal.

The main advantage of the proposed acquisition system is that surfaces can scanned with non-invasive procedures like painting. This is essential for applications like digitizing cultural heritage objects where no foreign substances should touch those precious artifacts. The second advantage is that by changing the light source alone, the other elements of the 3-D scanner are the same and do not need to be changed, making this solution cost-effective and simple.

A future work is to extend this technique to the acquisition of other materials with optically challenging surfaces, such as mirrors and liquids. We also planning to study the effect of the CCD sensitivity to UV-A and IR light to improve precision.

References

1. Chen, F., Brown, G.M., Song, M.: Overview of three-dimensional shape measurement using optical methods. Opt. Eng. **39**(1), 10–22 (2000)
2. Blais, F.: Review of 20 years of range sensor development. J. Electron. Imaging **13**(1), 231–243 (2004)
3. Ihrke, I., Kutulakos, K.N., Lensch, H.P.A., Magnor, M., Heidrich, W.: State of the art in transparent and specular object reconstruction. In STAR Proceedings of Eurographics, pp. 87–108 (2008)
4. Baba, M., Ohtani, K., Imai, M., Konishi, T.: New laser rangefinder for three-dimensional shape measurement of specular objects. Opt. Eng. **40**(1), 53–60 (2001)
5. Tarini, M., Lensch, H.P.A., Goesele, M., Seidel, H.P.: 3d acquisition of mirroring objects using striped patterns. Graph. Models **67**(4), 233–259 (2005)
6. Bonfort, T., Sturm, P., Gargallo, P.: General specular surface triangulation. Proceedings of the Asian Conference on Computer Vision, Hyderabad, India, vol. II, pp. 872–881 (2006)
7. Kutulakos, K.N., Steger, E.: A theory of refractive and specular 3d shape by light-path triangulation. Int. J. Comput. Vision **76**(1), 13–29 (2008)
8. Adato, Y., Vasilyev, Y., Zickler, T., Ben-Shahar, O.: Shape from specular flow. IEEE Transactions on Pattern Analysis and Machine Intelligence, **32**(11), 2054–2070 (2010)
9. Chuang, Y.Y., Zongker, D.E., Hindorff, J., Curless, B., Salesin, D.H., Szeliski, R.: Environment matting extensions: towards higher accuracy and real-time capture. In SIGGRAPH '00: Proceedings of the 27th annual conference on Computer graphics and interactive techniques, pp. 121–130 (2000)
10. Pulli, K.: Multiview registration for large data sets. In 3-D Digital Imaging and Modeling, 1999. Proceedings. Second International Conference on, pp. 160–168 (1999)
11. Rusinkiewicz, S., Levoy, M.: Efficient variants of the icp algorithm. In 3-D Digital Imaging and Modeling, 2001. Proceedings. Third International Conference, pp. 145–152 (2001)
12. Curless, B., Levoy, M.: A volumetric method for building complex models from range images. In SIGGRAPH '96: Proceedings of the 23rd annual conference on Computer graphics and interactive techniques, pp. 303–312. ACM, New York (1996)
13. Rocchini, C., Cignoni, P., Ganovelli, F., Montani, C., Pingi, P., Scopigno, R.: Marching intersections: an efficient resampling algorithm for surface management. In Shape Modeling and Applications, SMI 2001 International Conference on. pp. 296–305 (2001)
14. Cignoni, P., Montani, C., Scopigno, R.: A comparison of mesh simplification algorithms. Computers & Graphics **22**, 37–54 (1997)
15. Kutulakos, K.N., Steger, E.: A theory of refractive and specular 3d shape by light-path triangulation. **2**, 1448–1455 (2005)
16. Zongker, D.E., Werner, D.M., Curless, B., Salesin, D.H.: Environment matting and compositing. In SIGGRAPH '99: Proceedings of the 26th annual conference on Computer graphics and interactive techniques, pp. 205–214 (1999)
17. Park, J., Kak, A.C.: Multi-peak range imaging for accurate 3D reconstruction of specular objects. In: 6th Asian Conference on Computer Vision, Jeju, Korea, 27–30 Jan 2004, 6 pp (2004). http://cobweb.ecn.purdue.edu/RVL/Publications/Park
18. Park, J., Kak, A.C.: 3D modeling of optically challenging objects. IEEE Trans. Vis. Comput. Graph. **14**(2), 246–262 (2008)
19. Miyazaki, D., Kagesawa, M., Ikeuchi, K.: Transparent surface modeling from a pair of polarization images. IEEE Trans Pattern Anal. Mach Intell. **26**(1), 73–82 (2004)
20. Matusik, W., Pfister, H., Ziegler, R., Ngan, A., McMillan, L.: Acquisition and rendering of transparent and refractive objects. EGRW '02: Proceedings of the 13th Eurographics workshop on Rendering. pp. 267–278. Eurographics Association, Aire-la-Ville, (2002)
21. Ben-Ezra, M., Nayar, S.K.: What does motion reveal about transparency? IEEE Int. Conf. Comput. Vis. **2**, 1025 (2003)
22. Narita, D., Baba, M.: Measurement of 3-d shape and refractive index of a transparent object using laser rangefinder. Proceedings of the IEEE Conference on Instrumentation and Measurement Technology, 2005, vol. 3, pp. 2247–2252 (2005)
23. Chen, T., Lensch, H.P.A., Fuchs, C., Seidel, H.P.: Polarization and phase-shifting for 3d scanning of translucent objects. IEEE Conference on Computer Vision and Pattern Recognition, 2007. pp. 1–8 (2007)
24. Yamazaki, M., Iwata, S., Xu, G.: Dense 3d reconstruction of specular and transparent objects using stereo cameras and phase-shift method. In: ACCV (2), pp. 570–579 (2007)
25. Hullin, M.B., Fuchs, M., Ihrke, I., Seidel, H.P., Lensch, H.P.A.: Fluorescent immersion range scanning. ACM Trans. Graph. **27**(3), 1–10 (2008)
26. Besl, P.J.: Active, optical range imaging sensors. Mach. Vis. Appl. **1**(2), 127–152 (1988)
27. Masuda, T., Yokoya, N.: A robust method for registration and segmentation of multiple range images. In: Proceedings of the 1994 Second CAD-Based Vision Workshop. Champion, Pennsylvania, USA, 8–11 Feb 1994, pp. 106–113 (1994)
28. Hebert, M.: Active and passive range sensing for robotics. vol. 1, pp. 102–110 (2000)
29. Minolta: Non-contact 3D digitizer Vivid 9i/vi-9i. Instruction manual (hardware). Konica Minolta Sensing INC, 64 pp (2004). http://www.konicaminolta.com/content/download/4724/34935/VIVID910_VI-910.pdf
30. Cook, R.L., Torrance, K.E.: A reflectance model for computer graphics. ACM Trans. Graph. **1**(1), 7–24 (1982)
31. Zhang, R., Tsai, P.S., Cryer, J.E., Shah, M.: Shape-from-shading: a survey. IEEE Transactions on Pattern Analysis and Machine Intelligence **21**(8), 690–706 (1999)
32. Landsberg, G.S.: Optics. Ed. Mir, Moscow, USSR, 926 pp (1976)
33. Phalippou, J.: Verres. propriétés et applications. Techniques de l'ingénieur. Sciences fondamentales, 19 pp. Reference AF3601 (2001). http://www.techniques-ingenieur.fr/
34. Creasey, J., Tyrell, G., De Mattos, J.: Infrared camera with phosphor coated CCD. European patent: EP1199886, 5 pp (2004). http://www.freepatentsonline.com/EP1199886.pdf
35. Minoglou, K., De Munck, K., Tezcan, D.S., Van Hoof, C., De Moor, P., Bogaerts, J.: Backside illuminated thinned cmos image sensors for space imaging. In: IEEE Sensors, pp. 1429–1432 (2008)
36. Banpil Photonics: Expanding the boundaries of optics and electronics technologies: September (2010). http://banpil.com/mis.htm

Author Biographies

Maria Fernanda Osorio received a degree in Electronic Engineering in 2007 and MSc in Industrial Automation in 2010 both from the National University of Colombia at Manizales. Currently, she is an assitant instructor at the Catolica University at Manizales, Colombia.

Augusto Salazar received a degree in Electronic Engineering in 2004 and MSc in Industrial Automation in 2007, both from the National University of Colombia at Manizales. Currently, He is a PhD student in Engineering at the same University. His research has mostly been on

developing digital image processing techniques for 2D and 3D facial feature detection.

Flavio Prieto is professor at the Mechanical and Mecatronics Engineering Department at National University of Colombia. He received a degree in electronic engineering in 1991 from Francisco José de Caldas Distrital University, and his M.S. in electrical engineering in 1995 from Andes University, all in Bogotá, Colombia. He recived his PhD in 2000 in industrial automation from the Institut National des Sciences Appliquées de Lyon, France. His research interests include computer vision, image processing, automated inspection systems, and pattern recognition.

Pierre Boulanger worked for 18 years at the National Research Council of Canada as a senior research officer where his primary research interests were in 3D computer vision, rapid product development, and virtualized reality systems. He now holds a double appointment as a professor at the University of Alberta in the Department of Computing Science and in the Department of Radiology and Diagnostic Imaging, Faculty of Medicine and Dentistry.

Pablo Figueroa is an associate professor at the Computing Engineering and Systems Department at Universidad de los Andes, Colombia. His email ID is pfiguero@uniandes.edu.co.